forum acusticum 2026
8-12 September · Graz, Austria

AUTOMATIC THREE-DIMENSIONAL ACOUSTIC FIELD MAPPING FOR WATER TANK-BASED BIOACOUSTIC EXPERIMENTS

Ignasi Nou-Plana[1], Rachael Morgan[2], Augusto Fantinelli[1], Rosa Ma Alsina-Pagès[1]
[1] *Human-Environment Research (HER), La Salle - Universitat Ramon Llull, Barcelona, Spain*
[2] *Theoretical Ecology Group, University of Bergen, Bergen, Norway*

This paper is a revised version of the authors' submitted manuscript that was peer-reviewed by at least two anonymous reviewers.

Abstract

Laboratory water tanks are widely used to investigate the effects of underwater noise on aquatic organisms. However, small bounded volumes generate complex and highly reverberant acoustic fields, and the spatial distribution of sound inside experimental tanks is often insufficiently characterized prior to behavioural or physiological studies. As a result, the acoustic exposure experienced by organisms may vary significantly within the tank, introducing uncertainty in controlled noise experiments. This work presents an automated methodology for three-dimensional acoustic field mapping in laboratory tanks based on broadband impulse response measurements. A spatial scan is performed throughout the tank, and at each measurement position a broadband excitation signal is recorded and processed through deconvolution to estimate the impulse response. The methodology is applied to an experimental tank previously used for low-frequency and virtual reality exposure studies and the resulting dataset allows the spatial variability of the sound field within the tank to be assessed and provides a reproducible framework for tank calibration prior to bioacoustic experiments. This approach contributes to improving the reliability and interpretability of controlled underwater noise studies conducted in laboratory environments, focusing on fish or other marine organisms.

Keywords: *underwater acoustics, bioacoustics, acoustic field mapping, water tanks*

1. Introduction

Anthropogenic underwater noise is widely recognized as a growing environmental concern, with documented effects on fish communication, behaviour, and physiology [1], [2]. At the same time, large-scale monitoring initiatives and open datasets have improved the characterization of vessel noise and coastal soundscapes in European waters [3], [4]. While such efforts improve understanding of real-world acoustic environments, controlled laboratory experiments remain essential for assessing organismal responses under reproducible conditions. These experiments are frequently conducted in water tanks, where acoustic conditions differ fundamentally from open-water scenarios.

Small water tanks behave as bounded reverberant systems in which reflections at rigid walls and at the water–air interface generate modal patterns and strong spatial variability. The acoustics of small tanks have been recognized for several decades, with early foundational work describing the modal behaviour of confined water volumes [5]. Moreover, later studies have highlighted distortions and measurement uncertainties associated with confined environments [6], [7]. Under these conditions, sound pressure levels may vary substantially across spatial locations, raising concerns about the representativeness of single-point calibration approaches commonly used in biological experiments.

Analytical modelling of rectangular water-filled tanks has been addressed using modal formulations that account for boundary effects and structural leakage. In particular, [8] proposed a modal formulation capable of predicting normal frequencies and the spatial distribution of sound in rectangular tanks. More recently, combined theoretical predictions with robotic measurements to analyse the spatial distribution of normal modes in fish tanks is presented in [9], demonstrating the influence of frequency, water level, and measurement depth on acoustic uncertainty.

Despite these advances, many tank-based bioacoustic studies still rely on limited spatial sampling or calibration at selected reference points. For example, previous experimental work conducted in the same tank considered in this study employed a restricted

Corresponding author: *ignasi.nou@salle.url.edu.*

measurement grid and manual positioning to define an exposure location for low-frequency experiments [10], [11], [12].
The present work extends this by implementing an automated three-dimensional mapping methodology based on broadband impulse response measurements. By measuring the acoustic response at multiple locations throughout the tank, the proposed approach enables the spatial distribution of the sound field to be analysed across the measurement volume. This framework provides a reproducible basis for calibrating laboratory tanks used in bioacoustic experiments.

2. Experimental Tank and Context

The measurements presented in this work were conducted in a laboratory water tank previously used for controlled bioacoustic exposure experiments. The tank has internal dimensions of approximately $50 \times 50 \times 35$ cm and is made of 1 cm thick plexiglas walls filled with either freshwater or seawater. Such small laboratory tanks are commonly employed in experimental bioacoustics due to their accessibility and the ability to control environmental conditions.
Previous experiments performed in this tank focused on the study of biological responses to controlled underwater noise stimuli and visual stimuli. In those studies, the acoustic field was characterized using a limited number of measurement positions in order to define a reference exposure point within the tank [10]. While this approach improves repeatability at a specific location, it does not provide a complete description of the spatial acoustic variability inside the enclosure.

3. Measurement Methodology

3.1. Acoustic Excitation and Recording Chain

Acoustic measurements were performed using an underwater loudspeaker (AKUASOUND, Mausound) driven by a Behringer NX3000D Class-D power amplifier. The loudspeaker is an electrodynamic underwater transducer with a nominal impedance of 8 Ω and a maximum power rating of 100 W RMS, designed for broadband underwater sound generation.
The acoustic signal was recorded using an Aquarian AS-1 broadband hydrophone. The hydrophone provides an omnidirectional response and a linear frequency response in the range of 1 Hz to 100 kHz (± 2 dB), with a sensitivity of -208 dBV re 1 μPa.
Signal playback and acquisition were performed using a SpectraDAQ-200 data acquisition interface connected via USB. The interface provides 24-bit resolution and supports sampling rates up to 192 kHz. In the present study, measurements were recorded at a sampling rate of 44.1 kHz. Two input channels were used: one channel recorded the hydrophone signal, while the second channel recorded a loopback reference from the output signal. This configuration ensures precise synchronization between playback and recording signals during impulse response estimation.
The excitation signal consisted of an exponential sine

Figure 1: Experimental setup used for the automated acoustic measurements. The water tank is mounted within a rigid structural frame supporting a three-axis positioning system. The tank is mechanically suspended to reduce coupling with external vibrations, while the surrounding instrumentation enables synchronized signal playback and recording.

sweep ranging from 10 Hz to 10 kHz with a duration of 1.2 s. The sweep signal was generated digitally and reproduced through the underwater loudspeaker. All measurements were stored for offline post-processing.

3.2. Spatial Sampling

To characterize the acoustic field inside the tank, measurements were performed on a structured three-dimensional grid covering the accessible measurement volume. The underwater loudspeaker was suspended in the water near one side of the tank and remained fixed during the measurements. The hydrophone was mounted on a three-axis positioning system that moved it sequentially between measurement points.

The primary tank used in this study has internal dimensions of approximately $50 \times 50 \times 35$ cm and measurements were performed using a spatial resolution of 3 cm along each axis, resulting in a total of 910 measurement points within the accessible volume.

In addition to the main tank measurements, a secondary experiment was conducted using a smaller suspended enclosure with approximate dimensions of $20 \times 20 \times 20$ cm. Due to the effective water height and sensor geometry, the measurement region was restricted to approximately $16 \times 16 \times 12$ cm, resulting in a total of 180 measurement points. The same spatial resolution of 3 cm was used for these measurements.

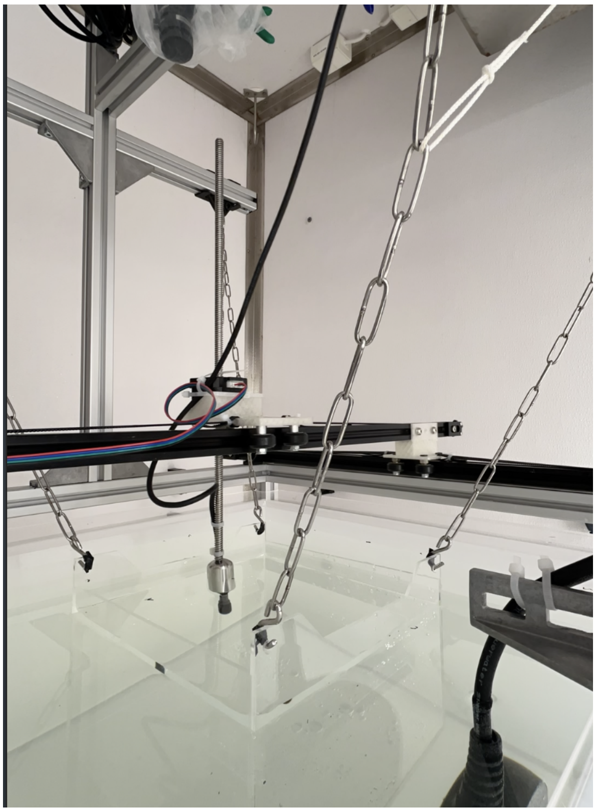

Figure 2: Detail of the positioning system inside the tank. The hydrophone is mounted on the vertical axis (z-axis), which is driven by a stepper motor mechanism allowing controlled positioning within the measurement volume. The structure enables repeatable and precise spatial sampling of the acoustic field.

3.3. Impulse Response Extraction

At each spatial coordinate, the exponential sine sweep was reproduced through the underwater loudspeaker while the hydrophone signal was recorded simultaneously with a loopback reference of the playback signal. The loopback channel provides a direct recording of the excitation signal as reproduced by the playback system and was used as the reference signal for the impulse response estimation. Impulse responses were estimated offline using frequency-domain deconvolution between the recorded hydrophone signal and the loopback reference and a regularized spectral division was applied to obtain a stable estimate of the transfer function between the loudspeaker and the hydrophone, the impulse response was then obtained through inverse Fourier transform of the resulting transfer function. To focus the analysis on the direct acoustic arrival and the early reflections, the impulse responses were windowed around the main peak of the signal. This processing was repeated for all measurement positions, producing a spatially indexed set of impulse responses across the scanned volume.

4. Automated 3D Mapping Framework

An automated three-dimensional measurement system was developed to characterize the acoustic field inside the tank. The system combines a motorized positioning mechanism for the hydrophone with synchronized signal playback and acquisition. As mentioned, the hydrophone was mounted on a three-axis Cartesian positioning system that moves the sensor sequentially between predefined spatial coordinates.

To minimize positioning time the grid was scanned using a serpentine scanning strategy. In this approach, the hydrophone moves along the x direction for each row of measurement points, reversing direction between consecutive rows while incrementing the y coordinate. Once a full horizontal plane is completed, the z coordinate is incremented and the process is repeated, reducing unnecessary repositioning movements.

The entire acquisition sequence was executed automatically using a custom Python control script that coordinated hydrophone positioning, signal playback, and data recording. The positioning system was controlled by a Raspberry Pi connected to a FlyD5 motor controller module driving the stepper motors of the three-axis positioning mechanism. The control script was executed on a separate computer that communicated with the Raspberry Pi to send positioning commands and manage the acquisition sequence, see Figure **??**.

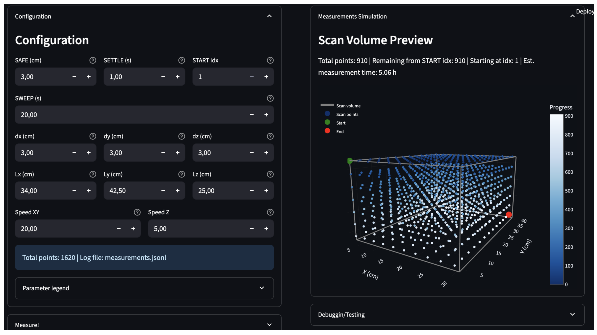

Figure 3: Graphical interface developed and used to configure and visualize the automated measurement procedure. The left panel allows the user to define scan parameters, including tank dimensions, safety margins, spatial resolution, and acquisition timing. The right panel provides a three-dimensional preview of the scan volume and measurement trajectory. The color gradient indicates the scan progression.

5. Preliminary Spatial Characterization

The automated measurement framework produces a spatial dataset of impulse responses throughout the tank volume. Preliminary results are shown in the following section, where these measurements are explored to illustrate the capabilities of the system and to highlight the spatial variability of the acoustic field inside the tank for these preliminary results.

5.1. Impulse Response Example

Figure 4 shows an impulse response measured at a representative position within the measurement region. The impulse response was obtained by deconvolving the recorded hydrophone signal using the simultaneously acquired loopback reference, which provides the excitation signal used for both temporal alignment and deconvolution.

The resulting signal exhibits an early arrival followed by a sequence of reflections originating from the tank boundaries, including the walls, bottom surface, and water–air interface. These contributions produce a decay characteristic of a reverberant environment. A prominent early arrival is observed at approximately 0.7 ms, corresponding to the direct acoustic path combined with a fixed system delay introduced by the acquisition chain. The absolute arrival time is therefore not interpreted in terms of propagation distance, but is used here to illustrate the temporal structure of the impulse response.

Such behaviour is expected in small bounded water volumes, where multiple reflections dominate the acoustic response. The impulse response reflects the complex propagation conditions within the tank, with successive arrivals associated with repeated boundary interactions.

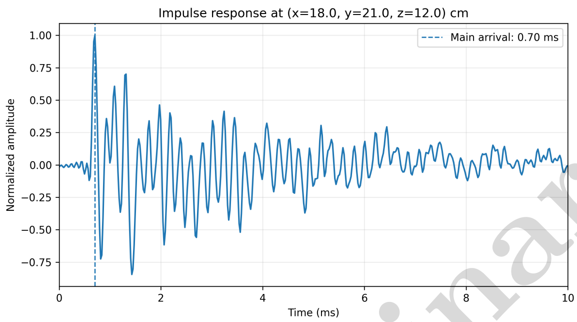

Figure 4: Impulse response measured at a representative position within the measurement region (x = 18.0 cm, y = 21.0 cm, z = 12.0 cm). A prominent early arrival is observed at approximately 0.7 ms, followed by multiple reflections from the tank boundaries, resulting in a prolonged decay characteristic of a highly reverberant bounded environment.

5.2. Frequency Response and Resonant Behaviour

The frequency response of the tank can be derived from the Fourier transform of the measured impulse responses. Figure 5 shows the magnitude spectrum obtained at the same representative position.

The spectrum shows pronounced peaks and notches across the analysed frequency range. These features come from constructive and destructive interference effects associated with the excitation of normal modes of the tank. This type of behaviour has been observed in previous studies on small water tanks, which have reported significant spectral irregularities and resonant effects in confined acoustic environments [5], [6], [9].

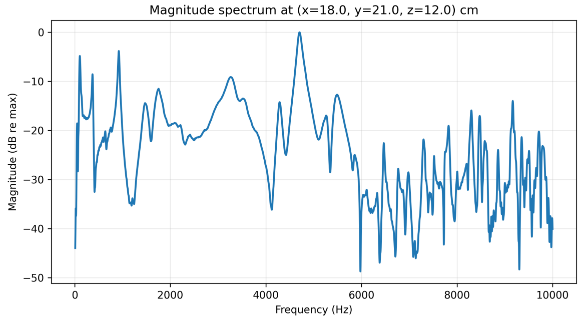

Figure 5: Magnitude spectrum derived from the impulse response at the same measurement position.

5.3. Spatial Variability of the Acoustic Field

One of the main advantages of the proposed measurement approach is the ability to evaluate the spatial variability of the acoustic field within the tank. By comparing impulse responses across the measurement grid, it is possible to observe differences in both amplitude and spectral content as a function of hydrophone position.

Figure 6 shows the spatial distribution of acoustic magnitude at two representative frequencies within the same horizontal measurement plane.

At low frequency (125 Hz), the acoustic field exhibits relatively smooth spatial variations across the measurement region. A clear amplitude gradient is observed, with higher levels closer to the loudspeaker, which is located near the right-hand side of the plots. This indicates that the field is largely dominated by direct propagation from the source, with limited spatial complexity due to the wavelength being large compared to the tank dimensions. The remaining asymmetry is primarily associated with the source position and boundary influences; asymmetrical positioning of the source within the tank, which contributes to the observed spatial gradient at low frequency.

At higher frequency (8000 Hz), the spatial distribution becomes significantly more irregular, with localized regions of higher and lower amplitude across the plane. Although the influence of the source position is still present, the field is now strongly shaped by interference effects and multiple reflections from the tank boundaries. This leads to a more complex and spatially heterogeneous acoustic field.

These results show the frequency dependence of spatial variability within the tank. While low frequencies produce smoother, source-dominated spatial patterns, higher frequencies give rise to increasingly structured fields due to the combined effects of interference and boundary interactions, highlighting the importance of frequency when interpreting acoustic measurements in water-tank environments.

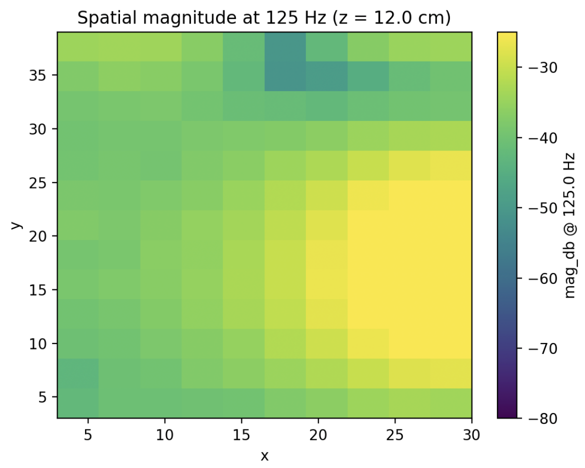

(a) Low frequency regime (125 Hz): smooth spatial variation dominated by direct propagation from the source

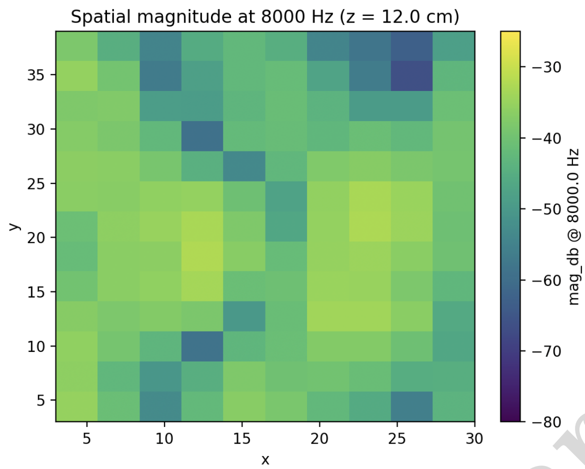

(b) High frequency regime (8000 Hz): increased spatial complexity due to interference and boundary reflections

Figure 6: Spatial distribution of acoustic magnitude within the same horizontal measurement plane at two representative frequencies. The loudspeaker is located near the right-hand side of the tank. At 125 Hz (top), the field exhibits relatively smooth spatial variations with a clear gradient increasing toward the source, indicating a dominant contribution from direct propagation. At 8000 Hz (bottom), the spatial pattern becomes more irregular, with localized amplitude variations due to stronger interference and boundary reflections.

6. Conclusions

The results presented in this study highlight the complex and strongly position-dependent nature of the acoustic field within small laboratory water tanks. The combination of broadband impulse response measurements and automated spatial sampling provides a detailed view of how acoustic energy is distributed throughout the tank volume.

The impulse response analysis confirms the highly reverberant character of the environment, with a prominent early arrival followed by a dense sequence of reflections, behaviour consistent with classical descriptions of small tank acoustics, where multiple boundary interactions dominate the sound field.

In the frequency domain, the presence of pronounced peaks and notches further supports the interpretation of the tank as a resonant system. These spectral irregularities are indicative of modal behaviour and interference effects arising from the tank geometry and boundary conditions.

The spatial analysis provides additional insight into how these effects manifest across the measurement volume. At low frequency, the acoustic field is largely dominated by direct propagation from the source, resulting in relatively smooth spatial variations with a clear dependence on source proximity. In contrast, at higher frequencies the field becomes increasingly heterogeneous, with localized regions of constructive and destructive interference. The results demonstrate that the acoustic exposure within the tank cannot be adequately described by a single measurement point. Even within a relatively small volume, substantial spatial variability is observed in both amplitude and spectral content. This has direct implications for bioacoustic experiments, where organisms may experience significantly different acoustic conditions depending on their position within the tank. The automated three-dimensional mapping framework presented in this work addresses this limitation by enabling systematic and reproducible characterization of the acoustic field. Compared to traditional manual measurements or sparse sampling approaches, the proposed method provides a volumetric dataset that captures both global trends and local variations. Moreover, the system is built from standard components, mainly based on CNC or 3D printers, with an estimated material cost below $400, making it accessible and easily reproducible in typical laboratory environments.

Despite these advantages, several limitations should be acknowledged. The measurements are influenced by the specific configuration of the experimental setup, including the position of the loudspeaker, the tank geometry, and the boundary conditions. As a result, the observed spatial patterns are not solely determined by intrinsic tank modes but also by source placement and experimental constraints. In addition, the analysis focuses on early impulse response components, which may not fully capture late reverberation effects. A constant delay between the loopback reference and the hydrophone channel might be observed, likely associated with the acquisition and signal routing chain. Although, this study represents an initial step on the proposed automated measurement framework, demonstrating the capability to capture the spatial and spectral complexity of the acoustic field within the tank.

Future work will focus on extending the analysis toward a more detailed characterization of modal behaviour and energy decay within the tank. The integration of these measurements with predictive acoustic models could further improve the understanding of sound propagation in confined water environments and support the design of more controlled bioacoustic experiments.

7. Acknowledgments

This work was supported by the European Molecular Biology Organization (EMBO) through a Scientific Exchange Grant (Grant No. 12181), which funded a research visit to the Theoretical Ecology Group at the University of Bergen.

References

[1] J. A. Hildebrand, "Anthropogenic and natural sources of ambient noise in the ocean," *Marine Ecology Progress Series*, vol. 395, pp. 5–20, 2009.

[2] A. N. Popper and A. D. Hawkins, "An overview of fish bioacoustics and the impacts of anthropogenic sounds on fishes," *Journal of fish biology*, vol. 94, no. 5, pp. 692–713, 2019.

[3] I. Nou-Plana, A. Teaca, F. Gazzada, M. Freixes, G. Zambon, and R. M. Alsina-Pages, "An open dataset for exploring underwater soundscapes and vessel noise in barcelona, constant, a and lagoon of venice basins," 2025.

[4] I. Nou-Plana, A. Teaca, G. Zambon, and R. M. Alsina-Pagès, "The deuteronoise dataset: An open, calibrated, multi-basin resource for vessel noise and natural soundscapes in european coastal waters," *Applied Acoustics*, vol. 246, p. 111 239, 2026.

[5] A. Parvulescu, "The acoustics of small tanks," 1967.

[6] T. Akamatsu, T. Okumura, N. Novarini, and H. Y. Yan, "Empirical refinements applicable to the recording of fish sounds in small tanks," *The Journal of the Acoustical Society of America*, vol. 112, no. 6, pp. 3073–3082, 2002.

[7] P. H. Rogers, A. D. Hawkins, A. N. Popper, R. R. Fay, and M. D. Gray, "Parvulescu revisited: Small tank acoustics for bioacousticians," in *The effects of noise on aquatic life II*, Springer, 2016, pp. 933–941.

[8] A. Novak, M. Bruneau, and P. Lotton, "Small-sized rectangular liquid-filled acoustical tank excitation: A modal approach including leakage through the walls," *Acta Acustica united with Acustica*, vol. 104, no. 4, pp. 586–596, 2018.

[9] J. Carbajo, P. Poveda, N. Ullah, and J. Ramis, "Acoustic analysis of fish tanks for marine bioacoustics research," *Journal of Marine Science and Engineering*, vol. 13, no. 7, p. 1253, 2025.

[10] M. Vidal, S. C. Mills, E. Gairin, F. Bertucci, and D. Lecchini, "Validation of a novel immersive virtual reality set-up with responses of wild-caught freely moving coral reef fish," *Animal Behaviour*, vol. 206, pp. 99–123, 2023.

[11] I. NOU PLANA et al., "Analysis of the underwater acoustic environment in the catalan shore: Badalona and port of barcelona cases in the framework of the deuteronoise jpi-oceans project," in *Inter-Noise and Noise-Con congress and conference proceedings*, Institute of Noise Control Engineering, vol. 270, 2024, pp. 216–227.

[12] I. Nou-Plana et al., "The deuteronoise dataset: An initial exploration of an underwater vessel sound dataset within the framework of a jpi-oceans project," *FRONTIERS IN ARTIFICIAL INTELLIGENCE AND APPLICATIONS*, vol. 390, pp. 260–269, 2024.